Effects of riblet surfaces on boundary-layer-induced surface pressure fluctuations and surface vibration

Nan Hu[1], Malte Misol[2]
[1] DLR, Institute of Aerodynamics and Flow Technology, Email: nan.hu@dlr.de
[2] DLR, Institute of Composite Structures and Adaptive Systems, Email: malte.misol@dlr.de

Abstract

Riblet surfaces are an effective means for drag reduction. The skin friction can be reduced by up to 10% with a dimensionless rib spacing in a range of about 14-18, applying the viscous length scale as normalization length. Apart from the drag reduction, the effect of riblet surfaces on surface pressure fluctuations and surface vibration might be of interest, especially for aircraft cabin noise. Experiments were performed at a plate configuration in the Acoustic Wind-Tunnel Braunschweig (AWB). Two riblet foils (102 μm and 150 μm rib spacing) and one foil without ribs but comparable mass were tested. The dimensionless rib spacing in the test is between 5 and 20.9. The results show no noticeable effect on the surface pressure fluctuations in the measurable frequency range (ca. 200 Hz-10 kHz) compared to the case without foils. However, riblet foils cause a vibration reduction of 1–2 dB compared to the foil without ribs. The greater stiffness of the riblet foils in the ribs direction might explain this behavior.

Experimental approach and results

The Acoustic Wind-Tunnel Braunschweig (AWB) is an open-jet low noise facility with a nozzle exit of 0.8 m x 1.2 m. The maximum flow velocity is 65 m/s. A 170 cm x 130 cm x 4 cm wood plate was aligned to the bottom side of the nozzle to allow boundary layer development, see figure 1. A 50 cm x 40 cm opening was realized at midspan in its rear portion for installation of aluminium test plates. Its rear edge is located 8 cm upstream of the rear edge of the wood plate. A 1 mm thick aluminium plate was applied for surface vibration measurements. A 6 mm thick aluminium plate was installed during flow measurements and surface pressure fluctuation measurements.

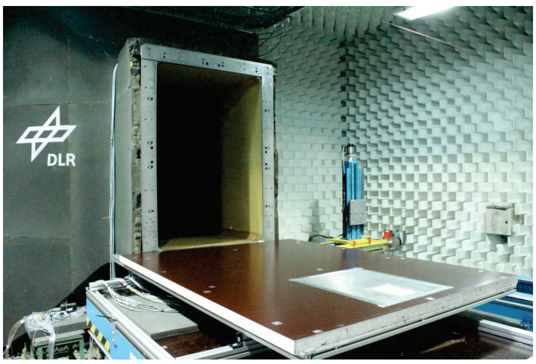

Figure 1: View of the experimental setup installed in AWB

Two different 3M sawtooth shaped riblet foils were tested. A schematic cross-sectional view is provided in figure 2. The rib spacing s was selected as 102 μm and 150 μm, respectively. Both riblet foil variants have a ridge angle of $\alpha = 53°$.

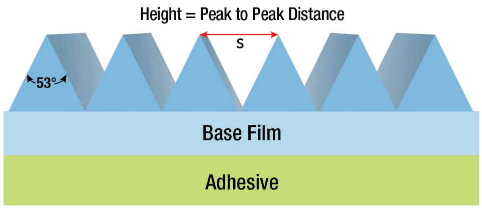

Figure 2: sketch of the tested riblet foils [1]

Flow measurements

The boundary layer flow field was measured by a single hotwire probe at 154 cm behind the nozzle exit at midspan of the reference plate without foils. Data were acquired at a sampling rate of 40 kHz for 13 s. Five different test velocities were set between 20.8 m/s and 62.4 m/s. The closest wall-normal distance from the probe to the plate surface for 20.8 m/s and 31.2 m/s was 1 mm and for the higher velocities 2 mm.

The friction velocity u_τ is obtained by fitting the measurement data to the logarithmic law of the wall. Figure 3 shows the mean flow profiles of the boundary layers for the different test velocities.

$$u^+ = \frac{1}{\kappa} \ln y^+ + C^+ \qquad (1)$$

where $u^+ = \frac{u}{u_\tau}$ and $y^+ = \frac{y u_\tau}{\nu}$. As genereally applied for smooth surfaces and zero pressure gradient boundary layers, the coefficients are herein set to $\kappa = 0.41$ (typical von Kármán constant) and $C^+ = 5.0$ [2].

The dimensionless rib spacing is defined as,

$$s^+ = \frac{s u_\tau}{\nu} \qquad (2)$$

The mean flow variables and the range of the dimensionless rib spacing for the tested riblet foils are listed in table 1. Bechert *et al.* [3] and Walsh [4] tested sawtooth shaped riblet foils with a similar ridge angle $\alpha = 54°$. A

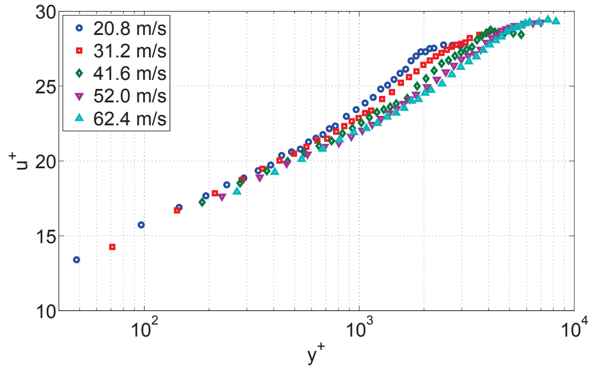

Figure 3: Logarithmic law plot of mean velocity profiles

drag reduction of more than 5% for $12 < s^+ < 18$ was reported. For a large $s^+ > 26$ the surface can be considered as a rough surface and the drag start to increase. For the present measurement, the whole tested range $5 < s^+ < 20.9$ is supposed to have a benefit of drag reduction.

Table 1: Boundary layer and riblet foil parameters

u_∞ (m/s)	δ (mm)	δ^* (mm)	u_τ	s^+(102μm/150μm)	Re_θ
20.8	45	7.00	0.75	5.0/7.5	7024
31.2	42	6.64	1.10	7.3/11.0	10191
41.6	42	6.21	1.44	9.6/14.4	12855
52.0	42	6.19	1.78	11.9/17.8	15904
62.4	41	5.90	2.09	13.9/20.9	18315

Surface pressure fluctuation measurements

Miniature piezo-resistive pressure sensors were used to measure surface pressure fluctuations. The sensor is from Entran, model EPE-S449-0.35B, with a diameter of 2.4 mm. Twelve sensors were flushmounted in a plastic plate with a size of 150 mm x 100 mm x 13 mm, fixed by rubber o-rings, illustrated in figure 4. An opening was made in the 6 mm aluminium plate to mount the plastic plate inserts. Data was sampled with 50 kHz for 30 s. A preamplifier with a high pass filter (cutoff frequency at 200 Hz) was used.

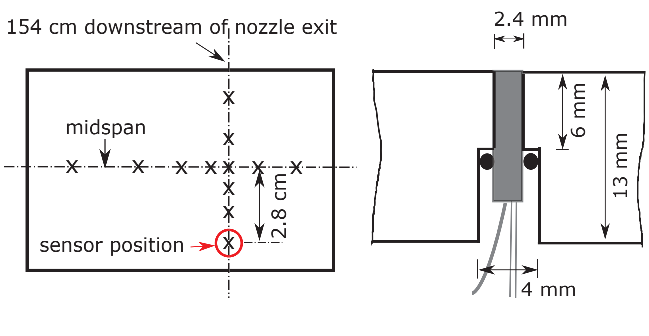

Figure 4: Schematic of sensor positions (left); sketch of the flushmounted sensor (right)

Measured power spectra for the marked sensor position in figure 4 at test velocities from 20.8 m/s to 62.4 m/s are shown in figure 5. Spectra have been corrected with the high pass filter correction curve down to 200 Hz. Spectra below 200 Hz are discarded due to the high background noise level especially at larger velocities and an increasing inaccuracy of the filter correction curve. Spectra at high frequencies e. g. from ca. 4 kHz for 20.8 m/s are contaminated due to electric disturbances or an imperfect surface transition between the sensor and the plastic plate surface. The spectra are uncontaminated up to ca. 10 kHz for large velocities 51.2 m/s and 62.4 m/s. Power spectrum level increases as the velocity increases. The maximum position is shifted to a higher frequency at a larger velocity. Measured spectra collapse perfectly by scaling for the test velocities, shown in figure 6. The maximum locates around $\omega\delta/U_\infty \approx 2$, which has been measured by several researchers [5].

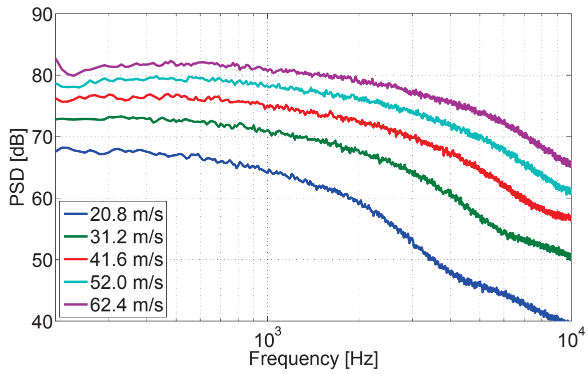

Figure 5: Power spectral density of surface pressure fluctuations for different velocities

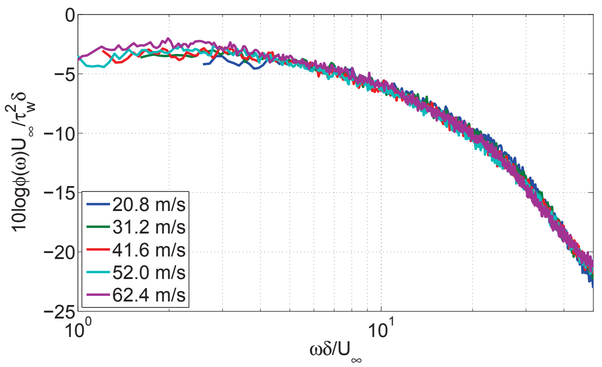

Figure 6: Spectra scaled by outer variables

Pressure fluctuations were measured on two riblet foils and one foil without ribs and compared to the reference case without foils. Foils with a length of 20 cm (ribs direction) and a width of 15 cm were pasted on the plate. A 2.4 mm hole at about 16.5 cm downstream of front edge was pierced on the foils using a sharped metal tube for placing the sensor. For the riblet foil test cases the ribs were aligned parallel to the flow. Special care was taken to mount the sensors flush to the surface of the base film (riblet foils) or to the surface (reference and foil without ribs). Measured pressure fluctuations show no noticeable difference between the reference case and the case with riblet foils or the foil with no ribs, shown in figure 7. Choi [6] measured surface pressure fluctuations on a riblet surface at a flow velocity $u_\infty = 3$ m/s and $\delta^* \approx 29.2$ mm. A remarkable pressure fluctuation reduction was found at frequencies below 20 Hz and a slight increase at frequencies between 20 Hz and 100 Hz. This trend is not observed in the present measurement. It should be noticed that any effect below 200 Hz cannot be evaluated with the current measurement setup.

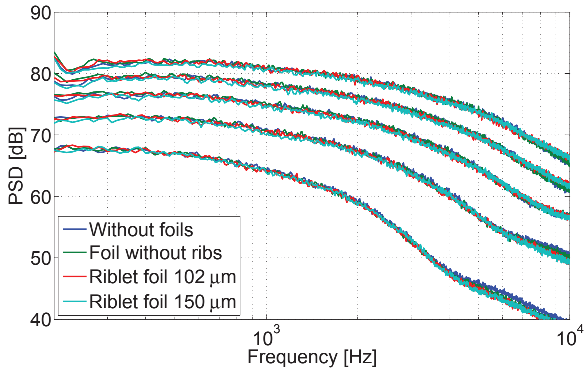

Figure 7: Comparison of surface pressure fluctuations

Surface vibration measurements

The 1 mm thick aluminium plate was inserted into the wood plate opening to measure the vibration response underneath the turbulent boundary layer. Thirty-five PCB (Model 352A24) miniature accelerometers were placed in a 5 x 7 matrix shape on the bottom side of the aluminium plate which enables to measure an averaged vibration characteristics over the whole plate, shown in figure 8. The accelerometer weight is 0.8 g and its dimensions in height, length and width are 4.8 mm, 12.7 mm and 7.1 mm. The measurement accuracy amounts 5% at 8 kHz and 10% at 10 kHz. Data was sampled at 20 kHz for 30 s. The bending wave wavelength of the aluminium plate at 10 kHz is ca. 31 mm which corresponds to the upper frequency limit of the applied sensor. The two riblet foils and the foil without ribs with a size of 47.5 cm x 37.5 cm were tested and compared to the case without foils. The foils have a similar weight of 49.2 g, 53.9 g and 56.1 g for the 102 μm riblet foil, the 150 μm riblet foil and the foil without ribs. The thicknesses of the foils are of the order of 250 μm.

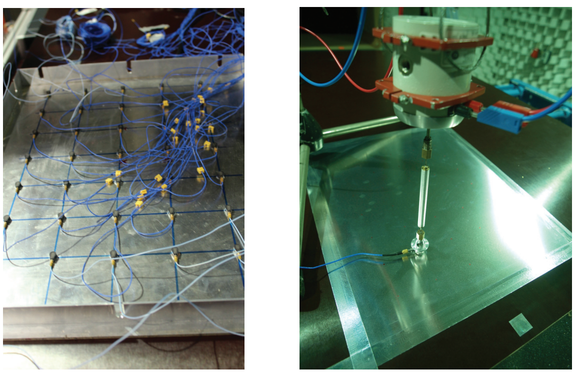

Figure 8: Position of accelerometers (left); view of the shaker excitation (right)

Transfer functions were measured for each case using a shaker excitation at a same location on the flow side, illustrated in figure 8 (right). For the case with foils the foil part at the shaker position was cut out, so that the shaker excitation was consistently applied on the aluminium plate. Measured transfer function spectra are shown in figure 9. The 1^{st} vibration mode of the aluminium plate is at about 55 Hz. Due to the additional mass of the foils the peaks shift to lower frequencies. A reduction of the transfer function levels is observed at high frequencies.

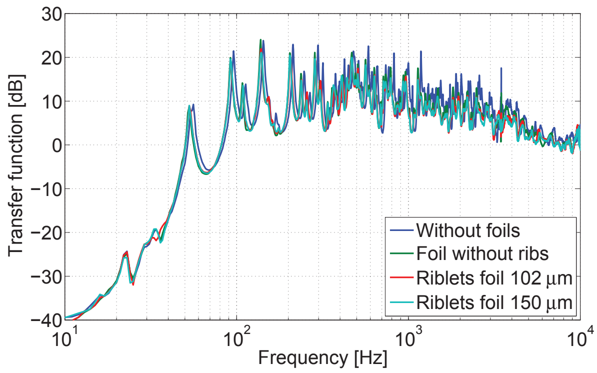

Figure 9: Comparison of averaged transfer function spectra for the shaker excitation

Measured boundary-layer-induced vibration spectra at 62.4 m/s were averaged by thirty-five accelerometers, shown in figure 10. A poor repeatability at high frequencies was obtained at lower velocities, which is probably due to a low signal to noise ratio. Peaks below 50 Hz are vibration modes from the wood plate, which is identified by an extra accelerometer placed on the wood plate. The high levels below 100 Hz are considered a specialty of the current test setup. In particular, the open-jet free shear-layers might lead to an additional vibration excitation of the wood plate. Moreover, also the hydrodynamic field at the midspan measurement position appears contaminated in this respective frequency range (range not included in figures 5 and 6). The vibration level decreases from 200 Hz to 2 kHz much faster than surface pressure fluctuations. It indicates a less effective transmission at higher frequencies for turbulent-boundary-layer-induced excitation, which is attributable to an increasing wavelength mismatch between surface pressure fluctuations and bending waves of the aluminium plate at higher frequencies. Particularly, the wavelength for surface pressure fluctuations decreases with $1/f$ but for bending waves of the aluminium plate with $1/\sqrt{f}$. Therefore, the wavelengths of the surface pressure fluctuations are much smaller than the bending wave wavelengths of the aluminium plate at higher frequencies, causing an inefficient transmission. The peaks shift to lower frequencies for cases with foils and the vibration reduction is larger at high frequencies. Similar trends were also observed in the transfer function measurement data.

1/3-octave band spectra show a clearer overview of the comparison between the different cases, shown in figures

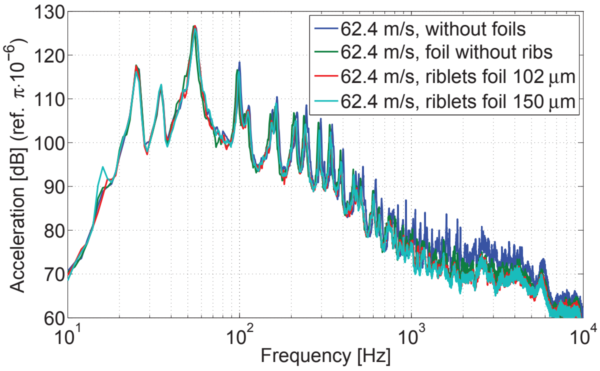

Figure 10: Comparison of averaged vibration spectra underneath the turbulent boundary layer

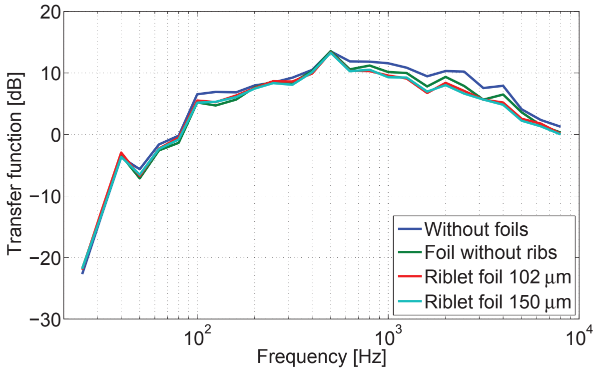

Figure 11: Comparison of averaged transfer function 1/3-octave band spectra for the shaker excitation

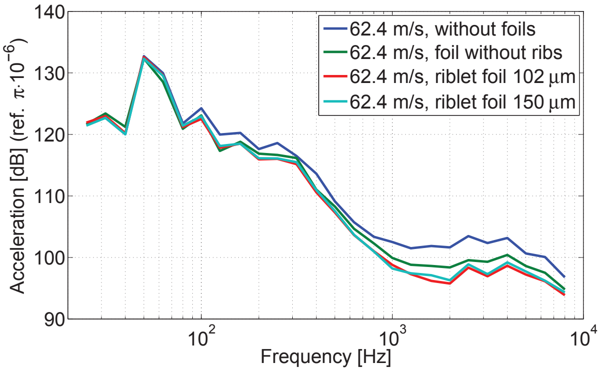

Figure 12: Comparison of averaged vibration 1/3-octave band spectra underneath turbulent boundary layer

11–12. The reduction of the transfer function levels is larger at high frequencies, i. e. up to 2 dB for the foil without ribs. Riblet foils show about 1 dB more reduction for frequencies larger than 700 Hz compared to the foil without ribs. The difference between the two riblet foil variants is small. Note that the weight of the foil without ribs is larger than for the two riblet foils, the reduced transfer efficiency could be due to a larger stiffness for the riblet foils in the rib direction than for the foil without ribs. The vibration induced by turbulent boundary layer shows a similar trend as the shaker excitation test. A broadband reduction up to 4 dB for the foil without ribs was measured. For riblet foils the reductions are larger and a maximum of 6 dB around 2 kHz was observed. Generally, the reduction for the cases with foils is larger underneath the turbulent boundary layer than using the shaker excitation. This might be explained by the two following aspects. First, transfer functions are different between shaker excitations and turbulent boundary layer excitations. Furthermore, only one excitation position was realized by the shaker, so several modes may not or weakly be excited, which is not the case for measurements underneath the turbulent boundary layer. Second, the surface texture might impact the transfer admittance for different test configurations.

It is also interesting to know how the riblet surface responses to the cases with ribs not aligned parallel to the flow. A 102 μm riblet foil (same size) with ribs 90° to the flow was tested. An 1–2 dB increase of vibrations was measured at high frequencies above 1 kHz and at low frequencies no remarkable difference was found, shown in figure 13. Even for this case with an imaginable negative impact on surface pressure fluctuations, the vibration is still slightly smaller than the case with the foil without ribs.

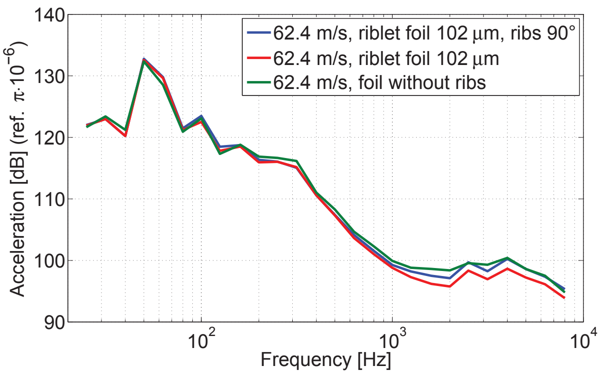

Figure 13: Comparison of averaged vibration 1/3-octave band spectra for the 102 μm riblet foil with ribs 90° to the flow

References

[1] 3M Poster, Riblet film for turbulence reduction, AWEA conference, 2011

[2] Schlichting, H. and Gersten, K., Boundary layer theory, Springer, New York, 2000

[3] Bechert, D.W., Bruse, M., Hage, W., van der Hoeven, J.G.T. and Hoppe, G., Experiments on drag-reducing surfaces and their optimization with an adjustable geometry, J. Fluid Mech., 1997

[4] Walsh, M.J., Turbulent boundary layer drag reduction using riblets, AIAA Paper 82-0169, 1982

[5] Goody, M, Empirical spectral model of surface pressure fluctuations, AIAA Journal, 2004

[6] Choi, K., Near-wall structure of a turbulent boundary layer with riblets, J. Fluid Mech., 1989